Quantum entanglement in the $S=1/2$ spin ladder with ring exchange

Jun-Liang Song, Shi-Jian Gu, and Hai-Qing Lin
Department of Physics and Institute of Theoretical Physics, The Chinese University of Hong Kong, Hong Kong, China
(Received 26 June 2006; published 23 October 2006)

In this paper we study the concurrence and the block-block entanglement in an $S=1/2$ spin ladder with four-spin ring exchange by the exact diagonalization method of finite clusters of spins. The relation between the global phase diagram and the ground-state entanglement is investigated. It is shown that block-block entanglement of different block sizes and geometry manifests richer information about the system. We find that the extremal point of the two-site block-block entanglement on the rung locates a transition point exactly due to SU(4) symmetry at this point. The scaling behavior of the block-block entanglement is discussed. Our results suggest that the block-block entanglement can be used as a convenient marker of the quantum phase transition in some complex spin systems.

DOI: 10.1103/PhysRevB.74.155119 PACS number(s): 03.67.Mn, 05.70.Jk, 75.10.Jm

I. INTRODUCTION

Entanglement, as one of the most intriguing feature of quantum mechanics,[1] has become a subject of intense interest in recent years. Besides being recognized as a crucial resource for quantum computing and quantum information processing,[2,3] it has also provided new perspectives in problems of various many-body systems. In particular, the entanglement can well characterize the features of the quantum phase transition (QPT).[4] Many works[5–19] have been devoted to understanding the relation between the QPT and entanglement in different systems. It has been observed that quantum phase transitions are signaled by critical behaviors of the concurrence,[20] a measure of entanglement for two-qubit systems, in a number of spin models.[5–9] For example, it was reported that the first derivative of the concurrence diverges at the transition point in the one-dimensional (1D) transverse field Ising model,[5] while the concurrence shows cusplike behavior around the critical point in some 2D and 3D spin models.[7] In addition to the concurrence, the block-block entanglement,[21] which involves more system degrees of freedom, was introduced.[12–14] Especially in fermionic systems in which the concurrence is usually not applicable, the block-block entanglement can also manifest interesting properties, such as logarithmic divergence in the critical region, in a certain class of models.[13,14]

However, most of the previous works on QPT and entanglement were restricted to models with two-body interactions; the models with three- or four-body interactions are less investigated,[22–24] and the connections between entanglement and novel phases brought about by these multispin interactions[25] are still less well understood by people. In fact a system with multibody interactions is important in both quantum information theory and condensed matter physics. It was pointed out that a small cluster of spins with three- or four-body interactions such as the four-spin ring exchange could be used for quantum computing.[26,27] Moreover, four-spin ring exchange exists in many physical systems and plays an important role in understanding the magnetism in several quantum systems such as solid ^{3}He (Ref. 28) and Wigner crystals.[29] Therefore, it is of importance to study the properties of the entanglement in those spin systems with multibody interactions.

In this paper, we consider a two-legged $S=1/2$ ladder with additional four-spin ring exchange. The system has a very rich phase diagram[25,30–33] with many exotic phases. We investigate the concurrence and the block-block entanglement in this system, and try to relate them to the global phase diagram. The rest of the paper is organized in the following way. In Sec. II, we introduce the model Hamiltonian and its phase diagram. In Sec. III, we study the ground-state concurrence and discuss its relation to the phase diagram. In Sec. IV, we show that the two-site block-block entanglement is exactly either maximal or minimal at a QPT point. In Sec. V, we show that the scaling behavior and some extremal point in the block-block entanglement can be used as markers of QPTs. In the final section, we summarize our results and draw conclusions.

II. MODEL HAMILTONIAN AND PHASE DIAGRAM

The two-legged $S=1/2$ spin ladder with ring exchange (as shown in Fig. 1) is described by the following Hamiltonian:

$$\hat{H} = J_r \sum_i \hat{S}_{1,i}\hat{S}_{2,i} + J_l \sum_i (\hat{S}_{1,i}\hat{S}_{1,i+1} + \hat{S}_{2,i}\hat{S}_{2,i+1}) + K \sum_i (\hat{P}_{i,i+1} + \hat{P}_{i,i+1}^{-1}), \quad (1)$$

where $i=1,\ldots,N/2$, N is the total number of spins, $\hat{S}_{1,i}$ ($\hat{S}_{2,i}$) is the spin-1/2 operator on the upper (lower) leg at the ith position, J_l (J_r) is the bilinear exchange constant along the legs (on the rung), and K is the coupling constant of the

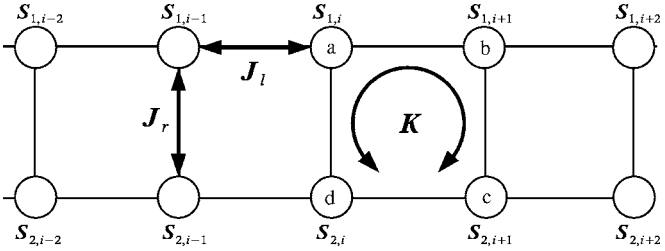

FIG. 1. Sketch of a spin ladder with ring exchange.

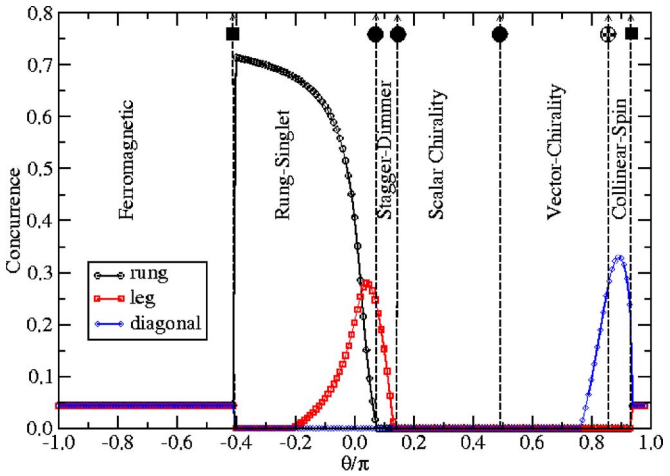

FIG. 2. (Color online) Ground-state concurrence of two spins on a rung, leg, and diagonal bond as a function of θ in an $N=12\times2$ spin ladder with ring exchange. The dashed lines are the boundaries of different phases. The squares on these lines denote a first-order phase transition, the black circles denote a second-order transistion, and the shaded circle indicates a transition between two adjacent regions.

four-spin cyclic exchange interaction $\hat{P}$. $\hat{P}_{i,i+1}$ ($\hat{P}_{i,i+1}^{-1}$) rotates the four-spin in the ith plaquette clockwise (counterclockwise) as shown in Fig. 1, i.e.,

$$\hat{P}\left|\begin{matrix} a & b \\ d & c \end{matrix}\right\rangle = \left|\begin{matrix} d & a \\ c & b \end{matrix}\right\rangle \quad \text{and} \quad \hat{P}^{-1}\left|\begin{matrix} a & b \\ d & c \end{matrix}\right\rangle = \left|\begin{matrix} b & c \\ a & d \end{matrix}\right\rangle,$$

and they can be decomposed in terms of spin operators involving bilinear and biquadratic terms,

$$\hat{P}+\hat{P}^{-1} = \frac{1}{4} + \hat{S}_a\hat{S}_b + \hat{S}_b\hat{S}_c + \hat{S}_c\hat{S}_d + \hat{S}_d\hat{S}_a + \hat{S}_a\hat{S}_c + \hat{S}_b\hat{S}_d + 4[(\hat{S}_a\hat{S}_b)(\hat{S}_c\hat{S}_d) + (\hat{S}_a\hat{S}_d)(\hat{S}_b\hat{S}_c) - (\hat{S}_a\hat{S}_c)(\hat{S}_b\hat{S}_d)]. \tag{2}$$

Following the convention in Ref. 25, we set $J_l=J_r=\cos\theta$ and $K=\sin\theta$ in the following calculation.

Previous studies[25] suggested a rich phase diagram in the parameter space of θ shown in Fig. 2. There are typically six phases (regions): the rung singlet phase, the staggered dimer phase, the scalar chirality phase, the dominant vector chirality region, the dominant collinear spin region, and the ferromagnetic phase. Squares in Fig. 2 denote first-order phase transitions, circles denote second-order phase transitions, and the dashed line indicates a crossover boundary without a phase transition.

Using the exact diagonalization method, we obtain the ground-state concurrence and the block-block entanglement in a spin ladder up to $N=12\times2$ sites with periodical boundary conditions. Although the staggered dimer and scalar chirality phases are Z_2 symmetry-breaking phases with double degeneracy in the thermodynamic limit, the ground state is unique for most values of θ except for the ferromagnetic phase in a finite-size system. We select the $S_z=0$ state out of the $(N+1)$-fold degenerate $S=N/2$ ferromagnetic states in the following calculation.

III. GROUND-STATE CONCURRENCE

The entanglement between the spins at site i and site j can be measured by the concurrence.[20] Let ρ_{ij} be the reduced density matrix, which is obtained by tracing out all degrees of freedom of spins except those of sites i and j, and $\tilde{\rho}_{ij}$ be the spin-flipped reduced density matrix of ρ_{ij}, i.e., $\tilde{\rho}=(\sigma_y\otimes\sigma_y)\rho^*(\sigma_y\otimes\sigma_y)$, where σ_y is the Pauli matrix. The concurrence C is given by $C=\max(\lambda_1-\lambda_2-\lambda_3-\lambda_4,0)$, where $\{\lambda_i\}$ are the square roots of the eigenvalues of the matrix $\rho\tilde{\rho}$ in descending order. $C=0$ means no entanglement, while $C=1$ corresponds to the maximum entanglement such as that in Bell states.

In Fig. 2 we show the ground-state concurrence as a function of θ for an $N=12\times2$ system. In the ferromagnetic phase, we can see that the concurrence on any two sites is the same and equals $1/(N-1)$. It vanishes in the thermodynamic limit $(N\to\infty)$. In the rung singlet phase, we can observe a rather large concurrence $(\theta\sim0.7\pi)$ between the two spins on the same rung. This fact is consistent with the picture that the ground state is approximated by the product state of spin singlets on the rungs. Similarly, the concurrence of two adjacent spins on the same leg is consistent with the physical picture of staggered singlets on the leg in the staggered dimer phase. We notice that the peak of concurrence on the leg (~0.3) is much smaller than that in the rung singlet phase (~0.7). This is because the ground state in the staggered dimer phase is twofold degenerate in the thermodynamic limit. Then in a finite-size system with periodic boundary conditions, the ground state is actually a superposition of these two states; thus the value of the concurrence on the leg reduces to one-half of the original value. In fact, if we impose boundary conditions in the same way as in Ref. 34, one of the two degenerate states will be projected out, a staggered pattern of the leg concurrence appears, and the value on the dimer leg is nearly 0.6, which is approaching the 0.7 in the rung singlet phase. In both the scalar chirality phase and dominant vector chirality phase, the concurrence of any pair of spin vanishes. However, at the crossover region between the dominant vector chirality and dominant collinear spin regions, an unexpected concurrence on the diagonal pair appears and its maximal point $(\theta\sim0.85\pi)$ is roughly the crossover point between the dominant vector chirality and dominant collinear spin regions.

IV. TWO-SITE ENTANGLEMENT OF THE RUNG AND THE SU(4) POINT

In this section and the following section, we study the block-block entanglement of various blocks in this system. The block-block entanglement is the von Neumann entropy E_v of a block of spin in the system. Precisely, it is calculated as

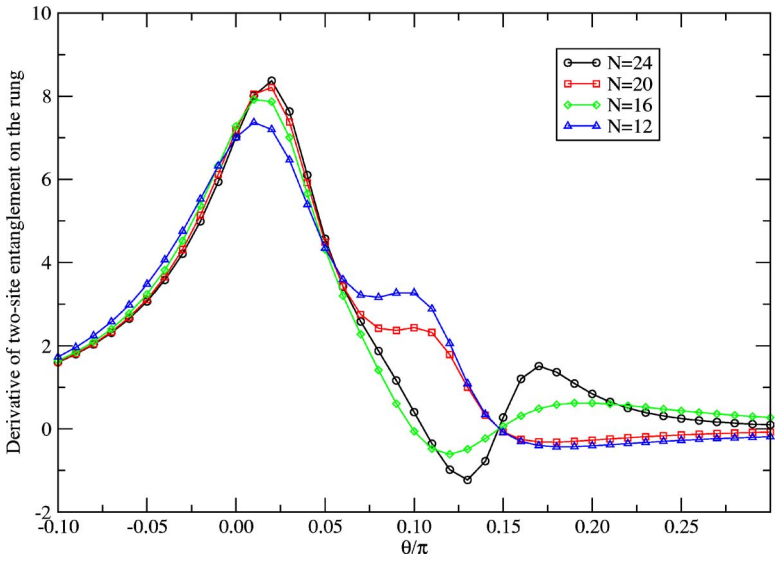

FIG. 3. (Color online) First derivative of the two-site entanglement on a rung as a function of θ. Lines of different system sizes cross at the same point $[\arctan(1/2),0]$.

$$E_v(A) = -\operatorname{tr}(\rho_A \log_2 \rho_A), \tag{3}$$

where A is a set of sites and ρ_A is the corresponding reduced density matrix. If the whole system is in a pure state, then

$$E_v(A) = E_v(B) = -\operatorname{tr}(\rho_B \log_2 \rho_B), \tag{4}$$

where B is the remainder of the system. Then $E_v(A)$ or $E_v(B)$ describes how much the block A and the rest of the system are entangled.

Compared to the concurrrence, the block-block entanglement can apply to systems with much higher degrees of freedom; however, it is meaningful only when the concerned state is a pure state. In our calculation of finite-size ladders, it is found that the ground state is always nondegenerate in the region $-0.40\pi < \theta < 0.95\pi$. Considering the SU(2) symmetry of the Hamiltonian, the ground state's total spin is also zero in this region.

The term "two-site entanglement" of a rung means that the von Neumann entropy is calculated from the reduced density matrix of two spins on the same rung. In Fig. 3 we show the first derivative of the entanglement as a function of θ for different system sizes. From the figure, we observe that the first derivative of the entanglement on a rung reaches zero exactly at $\theta=\arctan(1/2)\sim 0.148\pi$ which is the QPT point between the staggered dimer phase and the scalar chirality phase. We find that this result is independent of system size. Recently, it was pointed out that at this QPT point the system restores SU(4) symmetry.[31] Precisely speaking, at $\theta_c=\arctan(1/2)$, the Hamiltonian commutes with the following operator:[31]

$$\hat{T} = \sum_i \hat{S}_{1,i} \cdot \hat{S}_{2,i}. \tag{5}$$

We will show that the expectation value of $\hat{T}$ is maximal or minimal exactly at $\theta=\theta_c$ due to the above symmetry.

As discussed above, we can assume that the ground state $|\psi_0\rangle$ is nondegenerate around θ_c, which implies that $|\psi_0\rangle$ is also an eigenstate of $\hat{T}$ at θ_c; thus we have $\hat{T}|\psi_0\rangle=\lambda_t|\psi_0\rangle$ in which λ_t is some real number. Then the first derivative of $\langle\hat{T}\rangle$ with θ at θ_c is

$$\frac{d}{d\theta}\langle\psi_0|\hat{T}|\psi_0\rangle = \left\langle \frac{d\psi_0}{d\theta}\middle|\hat{T}\middle|\psi_0\right\rangle + \left\langle \psi_0\middle|\hat{T}\middle|\frac{d\psi_0}{d\theta}\right\rangle + \left\langle \psi_0\middle|\frac{d\hat{T}}{d\theta}\middle|\psi_0\right\rangle \tag{6}$$

$$= \lambda_t\left\langle \frac{d\psi_0}{d\theta}\middle|\psi_0\right\rangle + \lambda_t^*\left\langle \psi_0\middle|\frac{d\psi_0}{d\theta}\right\rangle + 0 = \lambda_t\frac{d}{d\theta}\langle\psi_0|\psi_0\rangle = 0. \tag{7}$$

Therefore, the expectation value of $\hat{T}$ reaches a local maximum or minimum at θ_c. Since the ground state has $(k_x,k_y)=(0,0)$, the system is invariant under translation along the leg, so $\langle\hat{S}_{1,i}\cdot\hat{S}_{2,i}\rangle=\langle\hat{S}_{1,j}\cdot\hat{S}_{2,j}\rangle$ (for any two sites i and j in the ladder) is either maximal or minimal at θ_c.

Next we show that there is one-to-one correspondence between $\langle\hat{S}_{1,i}\cdot\hat{S}_{2,i}\rangle$ and the two-site entanglement on the rung in the vicinity of θ_c. Let ρ_{ij} be the reduced density matrix of spins of sites i and j of the ground state. In the basis $\{|\downarrow\downarrow\rangle, |\downarrow\uparrow\rangle, |\uparrow\downarrow\rangle, |\uparrow\uparrow\rangle\}$, ρ_{ij} has the following form due to the U(1) symmetry of the ground state in the concerned region $(0.1\pi<\theta<0.2\pi)$:

$$\rho_{ij} = \begin{pmatrix} u^+ & 0 & 0 & 0 \\ 0 & w_1 & z^* & 0 \\ 0 & z & w_2 & 0 \\ 0 & 0 & 0 & u^- \end{pmatrix}. \tag{8}$$

Moreover, in the vicinity of $\theta=\theta_c$, the ground state is unique and its total spin $S=0$, which implies that the ground state is also invariant under any rotations. In particular, ρ_{ij} is invariant under rotation around the x axis:

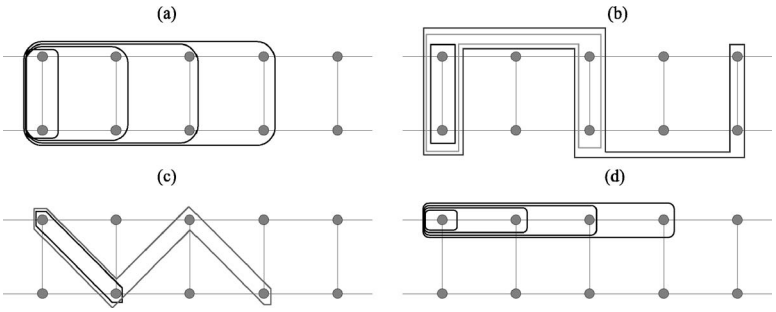

FIG. 4. Four choices for increasing the block size: (a) is the single block, (b) is the stripe block, (c) is the zigzag block, and (d) is the one-leg block.

$$[\sigma_i^x + \sigma_j^x, \rho_{ij}] = 0. \tag{9}$$

From Eq. (9) and the condition tr $\rho=1$, we have

$$u^+ = u^- = \frac{1+2z}{4}, \quad w_1 = w_2 = \frac{1-2z}{4}, \tag{10}$$

$$z = z^*, \quad \langle \hat{S}_{1,i} \cdot \hat{S}_{2,i} \rangle = -\frac{3z}{2}. \tag{11}$$

Then the block-block entanglement on the rung E_r is

$$E_r = -3u^+ \log_2 u^+ - (w_1 - z)\log_2(w_1 - z). \tag{12}$$

From the above equations it is clear that this extremal behavior of two-site entanglement on the rung is directly related to the SU(4) symmetry. It has been dicussed before that symmetries related to the QPT enter into entanglement functions for all system sizes, e.g., one-site entropy in the 1D Hubbard model at half filling with SO(4) symmetry at the metal-insulator transition.[15]

V. SCALING BEHAVIOR OF THE BLOCK-BLOCK ENTANGLEMENT

In this section, we focus on the scaling behavior of the block-block entanglement, namely, how the block-block entanglement behaves as the block size changes. Unlike the case of a one-dimensional chain, the ladder geometry has provided us many choices of how to select the block's shape and how to increase the block size. As shown in Fig. 4, we choose four different ways to increase the block size.

First, we notice that in the ferromagnetic phase, the value of the block-block entanglement depends only on the size of the block. It is independent of the block geometry. This is because any two sites in this state are essentially equivalent as we have already seen in Sec. III. In fact, an explicit expression of block-block entanglement as a function of block size l can be obtained in the following calculation.

The ferromagnetic $S^z_{tot}=\Sigma_i S^z_i=0$ state $\psi_{FM}(S^z_{tot}=0)$ could be obtained by applying a lowering operator on $\psi_{FM}(S^z_{tot}=N/2)$ $N/2$ times:

$$|\phi_{FM}(0)\rangle = \frac{\left(\sum_{i=1}^{N} \hat{S}_i^-\right)^{N/2}}{\sqrt{N!}} \underbrace{|\uparrow\uparrow\uparrow \ldots \uparrow\rangle}_{N}, \tag{13}$$

where $\hat{S}_i^-$ is the spin lowering operator at site i and N is the total number of sites. In the basis $\{|\downarrow\downarrow\rangle, |\downarrow\uparrow\rangle, |\uparrow\downarrow\rangle, |\uparrow\uparrow\rangle\}$, all the coefficients of $\psi_{FM}(S^z_{tot}=0)$ are the same: $\sqrt{(N/2)!(N/2)!/N!}$. The matrix element $\rho_l(p,q)$ can be obtained explicitly:

$$\rho_l(p,q) = \begin{cases} \dfrac{\left(\frac{N-l}{2}\right)!\left(\frac{N}{2}\right)!\left(\frac{N}{2}\right)!}{\left(\frac{N-l}{2}-p_z\right)!\left(\frac{N-l}{2}+p_z\right)!(N)!} & \text{if } p_z = q_z, \\ 0 & \text{if } p_z \neq q_z. \end{cases} \tag{14}$$

In the above expression, ρ_l is the reduced density matrix of the block consisting of l spins (we assume $l \leqslant N/2$), p and q are the column and row indices of ρ_l, and p_z and q_z are the corresponding S^z_{tot} numbers.

After diagonalizing this matrix, there are only $l+1$ nonzero eigenvalues λ_{p_z} with $p_z=-l/2,-l/2+1,\ldots,l/2$. Then the block-block entanglement can be obtained as

$$\lambda_{p_z} = \frac{(l)!\left(\frac{N-l}{2}\right)!\left(\frac{N}{2}\right)!\left(\frac{N}{2}\right)!}{\left(\frac{l}{2}-p_z\right)!\left(\frac{l}{2}+p_z\right)!\left(\frac{N-l}{2}-p_z\right)!\left(\frac{N-l}{2}+p_z\right)!(N)!},$$

$$E_v(l) = \sum_{p_z=-l/2}^{l/2} -\lambda_{p_z} \log_2 \lambda_{p_z}. \tag{15}$$

When l and N are large, the summation in Eq. (15) can be replaced by an integral, and the function λ_{p_z} can be approximated by a Gaussian distribution. Thus we can approximate $E_v(l)$ by the following expression:

$$E_v(l) \sim -\frac{1}{2}\log_2\left(\frac{1}{l}+\frac{1}{N-l}\right) + \frac{1}{2}\log_2\left(\frac{\pi e}{2}\right), \tag{16}$$

which suggests that $E_v(l)$ diverges logarithmically as the size l increases.

Second, in Fig. 5(a), in the largest region of the rung singlet phase, the block-block entanglement converges to some finite value quickly, while in Figs. 5(b)–5(d), it is almost proportional to the block size. Since the ground state is approximately the rung singlet product state, the block-block entanglement is proportional to the number of bonds crossing the boundary of the block as in Figs. 5(c) and 5(d). In Fig. 5(b), the situation is different since the number of bonds crossing the boundary of the block is finite the short-ranged

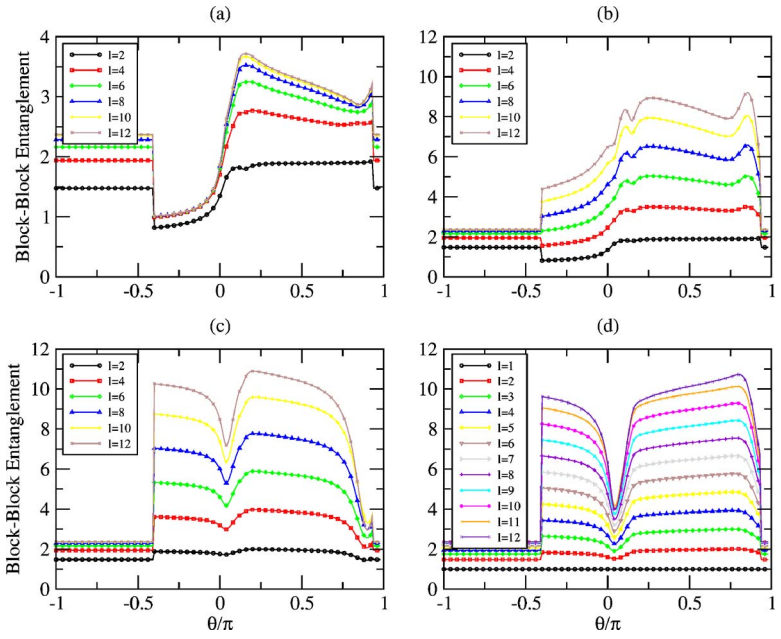

FIG. 5. (Color online) Block-block entanglement of different block sizes l as a function of θ in $N=12\times2$ ladder. The geometry of the blocks in (a), (b), (c), and (d) is specified in Figs. 4(a)–4(d).

correlations between the rungs play an important role in Fig. 5(b) and explain this proportionality. This result is in agreement with previous work,[35] i.e., the block entropy grows with the number of links going across the block interface area.

Next, in Figs. 5(b)–5(d), we find that some local extreme points of the block-block entanglement may be QPT points. Previous studies[25,31] suggested that the transition point between the rung singlet and staggered dimer is 0.06π–0.08π, which is quite near the local maximum point 0.07π in Fig. 5(b) and the local minimum 0.05π in Figs. 5(c) and 5(d). The transition point between the staggered dimer and scalar chirality phase is exactly 0.148π which is also near one minimal point 0.14π in Fig. 5(b). As for the crossover point between the dominant vector chirality region and the dominant collinear spin region, Figs. 5(b)–5(d) all suggest the value $\sim0.85\pi$ which is coincident with the value obtained in previous works.[25]

In general, the scaling behavior of the above four choices of blocks can be categorized into two kinds, Fig. 5(a) and Figs. 5(b)–5(d). In Fig. 5(a), the number of ladder bonds across the boundary between two blocks is a finite value 4 independent of the block size, while in Figs. 5(b)–5(d), the number is proportional to the block size l. In the latter case, the short-ranged correlation across the boundary bonds is the main contribution to the block-block entanglement; thus the block-block entanglement is always proportional to the size of the block as we have seen in Fig. 4. In the former case, the main contribution to the block-block entanglement comes from the long-range correlation between the sites in the block and the sites outside the blocks. It is expected that around the QPT point, in the former case the scaling behavior will change abruptly, e.g., from convergence to a finite value to logarithmic divergence, while in the latter case, there may exist an extremal point of the block-block entanglement, which is an indication of a QPT.

VI. SUMMARY

In summary, we have studied the concurrence and the block-block entanglement in the ground state of the $S=1/2$ spin ladder with ring exchange. In both the rung singlet and staggered dimer phases, the behaviors of the ground-state concurrence are consistent with the corresponding dominant configurations. The extremal point of the two-site block-block entanglement coincides with the QPT point due to the SU(4) symmetry, and this symmetry is obviously independent of the system size. We have also investigated the scaling behavior of the block-block entanglement for different block geometry and block sizes. We have identified three kinds of typical scaling behavior in this model, namely, on increasing the size of the block, the block-block entanglement (a) converges to some finite value, (b) diverges logarithmically with size, on (c) diverges proportionally with the size. However, we can see that there is no signature of the QPT between the scalar chirality phase and dominant vector chirality phase.

ACKNOWLEDGMENTS

This work is supported by an Earmarked Grant for Research from the Research Grants Council of HKSAR, China (Projects No. N_CUHK204/05 and No. HKU_3/05C).

[1] A. Einstein, B. Podolsky, and N. Rosen, Phys. Rev. **47**, 777 (1935).
[2] C. Bennett and D. Divincenzo, Nature (London) **404**, 247 (2000).
[3] M. Nielsen and I. Chuang, *Quantum Computation and Quantum Information* (Cambridge University Press, Cambridge, U.K., 2000).
[4] S. Sachdev, *Quantum Phase Transitions* (Cambridge University Press, Cambridge, U.K., 2000).
[5] A. Osterloh, L. Amico, G. Falci, and Rosario Fazio, Nature (London) **416**, 608 (2002).
[6] T. J. Osborne and M. A. Nielsen, Phys. Rev. A **66**, 032110 (2002).
[7] S. J. Gu, H. Q. Lin, and Y. Q. Li, Phys. Rev. A **68**, 042330 (2003); S. J. Gu, G. S. Tian, and H. Q. Lin, *ibid.* **71**, 052322 (2005).
[8] R. G. Unanyan, C. Ionescu, and M. Fleischhauer, Phys. Rev. A **72**, 022326 (2005).
[9] J. Vidal, Phys. Rev. A **73**, 062318 (2006).
[10] S. Yi and H. Pu, Phys. Rev. A **73**, 023602 (2006).
[11] X. F. Qian, T. Shi, Y. Li, Z. Song, and C. P. Sun, Phys. Rev. A **72**, 012333 (2005).
[12] S. J. Gu, G. S. Tian, and H. Q. Lin, New J. Phys. **8**, 61 (2006).
[13] G. Vidal, J. I. Latorre, E. Rico, and A. Kitaev, Phys. Rev. Lett. **90**, 227902 (2003).
[14] V. E. Korepin, Phys. Rev. Lett. **92**, 096402 (2004).
[15] S. J. Gu, S. S. Deng, Y. Q. Li, and H. Q. Lin, Phys. Rev. Lett. **93**, 086402 (2004); S. S. Deng, S. J. Gu, and H. Q. Lin, Phys. Rev. B **74**, 045103 (2006).
[16] D. Larsson and H. Johannesson, Phys. Rev. Lett. **95**, 196406 (2005).
[17] Ö. Legeza and J. Sólyom, Phys. Rev. Lett. **96**, 116401 (2006).
[18] A. Anfossi, P. Giorda, A. Montorsi, and F. Traversa, Phys. Rev. Lett. **95**, 056402 (2005); A. Anfossi, C. Degli Esposti Boschi, A. Montorsi, and F. Ortolani, Phys. Rev. B **73**, 085113 (2006).
[19] L. Campos Venuti, C. Degli Esposti Boschi, M. Roncaglia, and A. Scaramucci, Phys. Rev. A **73**, 010303(R) (2006).
[20] W. K. Wootters, Phys. Rev. Lett. **80**, 2245 (1998).
[21] K. Audenaert, J. Eisert, M. B. Plenio, and R. F. Werner, Phys. Rev. A **66**, 042327 (2002).
[22] Indrani Bose and Amit Tribedi, Phys. Rev. A **72**, 022314 (2005).
[23] J. Rissler, R. Noack, and S. White, Chem. Phys. **122**, 024107 (2005).
[24] Ö. Legeza and J. Sólyom, Phys. Rev. B **68**, 195116 (2003).
[25] A. Läuchli, G. Schmid, and M. Troyer, Phys. Rev. B **67**, 100409(R) (2003).
[26] A. Mizel and D. A. Lidar, Phys. Rev. Lett. **92**, 077903 (2004).
[27] V. W. Scarola, K. Park, and S. Das Sarma, Phys. Rev. Lett. **93**, 120503 (2004).
[28] M. Roger, C. Bäerle, Yu. M. Bunkov, A. S. Chen, and H. Godfrin, Phys. Rev. Lett. **80**, 1308 (1998).
[29] T. Okamoto and S. Kawaji, Phys. Rev. B **57**, 9097 (1998).
[30] M. Müller, T. Vekua, and H. J. Mikeska, Phys. Rev. B **66**, 134423 (2002).
[31] T. Hikihara, T. Momoi, and Xiao Hu, Phys. Rev. Lett. **90**, 087204 (2003).
[32] S. Brehmer, H. J. Mikeska, M. Müller, N. Nagaosa, and S. Uchida, Phys. Rev. B **60**, 329 (1999).
[33] Ö. Legeza, G. Fáth, and J. Sólyom, Phys. Rev. B **55**, 291 (1997).
[34] T. Hakobyan, J. H. Hetherington, and M. Roger, Phys. Rev. B **63**, 144433 (2001).
[35] Ö. Legeza, F. Gebhard, and J. Rissler, cond-mat/0512270.